16TH EUROPEAN CONFERENCE ON EARTHQUAKE ENGINEERING THESSALONIKI 18 - 21 JUNE 2018

ASSESSMENT OF RESIDUAL CAPACITY AND FRAGILITY-BASED FATIGUE OF CONCRETE STRUCTURES ACROSS MULTIPLE EARTHQUAKES FROM THE CANTERBURY EARTHQUAKES IN NEW ZEALAND

John B. MANDER[1], Geoffrey W. RODGERS[2], David WHITTAKER[3]

ABSTRACT

The Canterbury earthquake and aftershock sequence in New Zealand during 2010-2011 subjected the city's structures to a significant accumulated cyclic demand and raised significant questions regarding the low-cycle fatigue demands imposed upon the structures. There is a significant challenge to quantify the level of cumulative demand imposed on structures and to assess the percentage of a structure's fatigue life that has been consumed as a result of this earthquake sequence. It is important to be able to quantify the cumulative demand to determine how a building will perform in a subsequent large earthquake and inform repair and re-occupancy decisions.

This paper investigates the cumulative fatigue demand for a structure located within the Christchurch Central Business District (CBD). Time history analysis and equivalent cycle counting methods are applied across the Canterbury earthquake sequence, using key events from September 4th 2010 and February 22nd, 2011 main shocks. The estimate of the cumulative fatigue demand is then compared to the expected capacity of a case study reinforced concrete bridge pier, to undertake a structure-specific fatigue assessment. The analysis is undertaken to approximate the portion of the structural fatigue capacity that has been consumed, and how much residual capacity remains.

Results are assessed for recordings at the four Christchurch central city strong motion recording sites installed by the GeoNet programme, to provide an estimate of variation in results. The computed cyclic demand results are compared to code-based design methods and as assessment of the inelastic displacement demand of the reinforcing steel. Results are also presented in a fragility context where a de minimis (inconsequential), irreparable damage and full fatigue fracture are defined to provide a probabilistic assessment of the fatigue damage incurred. This methodology can provide input into the overall assessment of fatigue demands and residual capacity.

Keywords: Fatigue; Earthquake Damage; Residual Capacity; Fragility.

1. INTRODUCTION

Large earthquakes induce a number of cycles of vibration of varying amplitude. Particularly under inelastic seismic response, such vibrations cause progressive damage and deterioration of resistance. Moreover, even a moderate level earthquake may also strain the reinforcing steel beyond its elastic limit thereby causing yield and permanent damage. As mild steel reinforcing bars generally possess a large reserve (monotonic) strain capacity, one-time yielding is generally not considered a serious issue. However, if the structure has sustained several post-yield cycles of loading, even though the concrete may be repairable, there remains substantial seismic induced fatigue damage to the reinforcing steel. Although restoration is required, seismic-induced fatigue damage to reinforcing steel is generally irreparable; the phenomenon is known as 'low cycle fatigue', representing a low number of large strain amplitude cycles.

[1]Zachry Professor, Civil Engineering, Texas A&M University, College Station, USA, jmander@civil.tamu.edu
[2]Associate Professor, Mechanical Engineering, University of Canterbury, Christchurch, New Zealand, geoff.rodgers@canterbury.ac.nz
[3]Technical Director, Structural Engineering, Beca, Christchurch, New Zealand, david.whittaker@beca.com

While modern seismic loading codes carefully consider the onset of plastic deformation within a structure and provide levels of acceptable damage through limit states design, the long-term implications of such expected damage, in terms of cyclic fatigue failure, are not well considered. Structural fatigue considerations have been highlighted most recently in the Canterbury region of New Zealand, where an atypically long earthquake and aftershock sequence has placed significant cyclic demands on the region's structures. The post-earthquake restoration of damaged structures requires an assessment of the degree of damage sustained and measures whereby the structure may be restored to a substantially as new condition.

This paper presents an investigation into the cumulative cyclic fatigue demand imposed upon a bridge pier structure during the 2010-2011 Canterbury (New Zealand) earthquake and aftershock sequence for the Christchurch CBD. A composite spectra equal to the median response of all four strong motion recording stations within the CBD is used to represent the ground shaking intensity. Estimates of the cumulative fatigue demand across the all major events from the 2010-2011 Canterbury Earthquake Sequence are assessed and compared with the cyclic fatigue capacity of a bridge pier that has been designed to New Zealand standards.

2. METHODS

2.1 Assessment of Structural Fatigue Capacity

Low cycle fatigue results from Mander et al. (1994) show for both mild steel reinforcing bars and for high-strength high-alloy prestressing threadbars (f_y= 870 MPa yield strength), a general fatigue-life relationship may be given by:

$$\varepsilon_{ap} = 0.08(2N_f)^{-0.5} \tag{1}$$

The inverse of the number of cycles to failure (N_f), may be defined as the fatigue damage for one cycle of loading at the plastic strain amplitude (ε_{ap}), thus $D_{cycle} = 1/N_f$. Therefore, inverting Equation (1) and generalizing the result one obtains

$$D_{cycle} = \frac{1}{N_f} = \left|\frac{\varepsilon_{ap}}{\varepsilon_{pf}}\right|^2 \tag{2}$$

in which $\varepsilon_{pf} =$ is defined as the plastic fatigue strain (the plastic strain that would lead to only one cycle of fully reversed loading for fracture to occur), where for reinforcing steel this strain has a value in the range of $\varepsilon_{pf} = 0.06$ to 0.083 as shown by the results plotted in Figure 1. The variability in the results can also be represented by a lognormal distribution with a lognormal standard deviation of 0.25.

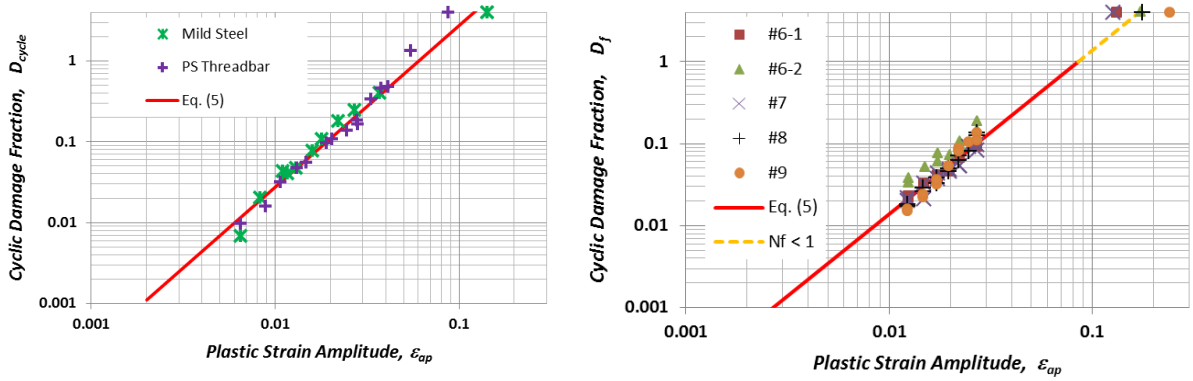

(a) $\varepsilon_{pf} = 0.06$ *from test results in Mander et al. (1994).*

(b) $\varepsilon_{pf} = 0.083$ *from test results in Brown and Kunnath (2004)*

Figure 1. Fatigue damage modelling based on tests from two different sources.

The damage model in Eq. (2) can be generalized to incorporate multiple cycles of constant amplitude loading, or variable amplitude loading. If D_{cycle} is the damage incurred by one completely reversed cycle of loading for a specific cyclic amplitude, and if multiple random cycles exist, then Miner's hypothesis may be used to estimate the cumulative fatigue damage fraction (D_f). The total damage may be found by norming all partial damage cycles to the maximum strain amplitude, and converting the total number of cycles into an effective number of constant amplitude cycles of loading (N_{eff}) whereby there is damage equivalence between the constant amplitude cycles and variable amplitude cycles:

$$D_f = \sum D_i = \sum \left|\frac{\varepsilon_{ap}}{\varepsilon_{pf}}\right|_i^2 = N_{eff} \left|\frac{\varepsilon_{pm}}{\varepsilon_{pf}}\right|^2 \quad (3)$$

in which $\sum D_i =$ summation of damage fractions for each of the i^{th} cycles; $N_{eff} =$ the equivalent/effective number of constant amplitude cycles which is based on $\varepsilon_{pm} =$ the peak plastic strain response for the loading history under consideration.

A reinforced concrete structure under dynamic excitation, will respond to the overall excitation from the foundation upwards—the foundation dynamically loads the structure as a whole, and the structural members resist the imposed loading. Large seismic loads induce *plastic displacements* in the structural members, which in turn produce *plastic rotations* within the plastic hinge zones that in turn result in *plastic curvatures* at the critical region of the plastic hinge, which finally cause *plastic strains* in the reinforcing bars at those critical hinge locations. The connection between plastic displacements, rotations, curvatures and strains can be related via geometric transformations, as given below. Therefore, Eq. (3) may be expanded accordingly as follows:

$$D_f = N_{eff} \left|\frac{\varepsilon_{pm}}{\varepsilon_{pf}}\right|^2 = N_{eff} \left|\frac{\phi_{pm}}{\phi_{pf}}\right|^2 = N_{eff} \left|\frac{\theta_{pm}}{\theta_{pf}}\right|^2 = N_{eff} \left|\frac{\Delta_{pm}}{\Delta_{pf}}\right|^2 \quad (4)$$

in which ϕ_{pm}, θ_{pm}, Δ_{pm} are the maximum peak curvature, rotation and displacement response values for the load history under consideration, and ϕ_{pf}, θ_{pf}, Δ_{pf} are the curvature, rotation and displacement parameters that are equivalent to a response that would lead to fatigue failure with only one completely reversed cycle of loading, $N_f = 1.0$ in Eq. (2).

The parameters ε_{pf}, ϕ_{pf}, θ_{pf}, Δ_{pf} are interconnected via characteristic structural geometry attributes, the latter three of which are structure-specific. The evaluation of such parameters is considered in the following subsections in which relationships are developed starting from bar strain and subsequently transformed to global structure displacement.

For a structure that essentially behaves in a single degree of freedom fashion, such as the bridge presented in Figure 2, plastic strains and curvatures are connected by (Dutta and Mander, 2001):

$$\phi_p = 2\varepsilon_{ap}/D' \quad (5)$$

where $D' =$ the pitch circle diameter of the longitudinal reinforcement in the bridge pier.

Plastic hinge rotations are connected to the plastic curvatures by:

$$\theta_p = \phi_p L_p \quad (6)$$

in which $L_p =$ the equivalent plastic hinge length given by:

$$L_p = 0.08\, L + 4400\, \varepsilon_y\, d_b \quad (7)$$

where $L =$ the column length; $\varepsilon_y =$ yield strain of the longitudinal reinforcement; and $d_b =$ diameter of the longitudinal bars.

The plastic displacement (drift) can be related to the plastic rotation of the column:

$$\Delta_p = \theta_p \, h_e \tag{8}$$

where h_e = height to the seismic centre of mass.

2.2 Assessment of Structural Fatigue Demand

Several methods are available for to convert each displacement response into equivalent constant amplitude fatigue cycles. Rain-flow methods are commonly used to decompose a random response into a number of different amplitude-specific blocks of different mean stress for high cycle fatigue with non-zero mean stress. Chang and Mander (1994) developed energy-based cycle counting methods suited to inelastic spectra analysis and the energy-based fatigue rules given in Mander et al. (1994). Neither are applicable for the elastic spectra developed herein, instead two simple methods were investigated.

A normalization routine, referred to herein as RMC, where RM means "root mean" and $C = -1/c$ in which c = the fatigue exponent that controls the relative importance placed on different amplitude response cycles, similar to a classic "peak picking" method, where each identified positive and negative peak is amplitude weighted to the power of C. The underlying principle is that the damage done by the variable amplitude loading is equivalent to an effective number of cycles N_{eff} for the maximum amplitude, in the present context this is the spectral displacement, S_d.

From Eq. (3), it follows that $D_{const} = \sum D_i$, where D_{const} = the damage by constant amplitude cycling; and $\sum D_j$ = summation of damage fractions of the peaks for the variable amplitude history. Expanding in terms of individual peaks:

$$2N_{eff} \left|\frac{S_d}{S_u}\right|^C = \sum \left|\frac{X_j}{S_u}\right|^C \tag{9}$$

where $2N_{eff}$ = the number of peaks/reversals in the history; S_u = the ultimate displacement peak for $N_{eff} = 1$; and X_j = the amplitude of the j^{th} peak of the random history. Thus the effective number of constant amplitude cycles is N_{eff}. To reduce the computational overhead of counting peaks, a more expedient approach is to consider every point, X_j, in the displacement history and correct for the fact that not all points are considered at the peak, giving this formulation for cycle counting:

$$N_{eff} = \frac{1}{2}\sum \left|\frac{X_j}{S_d}\right|^C = \frac{\Delta t}{T}\sum \left|\frac{B_c \, X_i}{S_d}\right|^C \tag{10}$$

in which Δt = the time-step length used in the elastic earthquake time-history analysis; T = the natural period of vibration for the case under consideration ($T/\Delta t$ = the number of points in one cycle of motion); and B_c = the amplification factor, dependent on the exponent C such that one-cycle of constant amplitude motion gives a result of unity. For exponent values of C = 1, 2, 3, the amplification factors are $B_{c=1} = \pi/2$, $B_{c=2} = \sqrt{2}$, and $B_{c=3} = 4/3$, respectively. For reinforcing-steel critical fatigue, C = 2. This approach is identical to the well-known root-mean-square (RMS) signal analysis technique. The cycle counting approach used herein is a development of, but remains similar to, that given in Dutta and Mander (2001).

2.2 Bridge Pier Case Study Structure

Figure 2 presents details of a bridge pier designed (Tanabe, 1999) conforming to New Zealand code requirements. The pier is 7 m high and is taken from a "long" multi-span highway bridge on firm soil with 40 m longitudinal span and 10 m transverse width. The weight of the super-structure reaction at each pier is assumed to be 7,000 kN. The bridge was designed for an earthquake with a spectral acceleration of 0.4g. This bridge has been the subject of previous studies on financial losses (Dhakal and Mander, 2006). It is used as a case study structure and re-examined here for seismic fatigue damage.

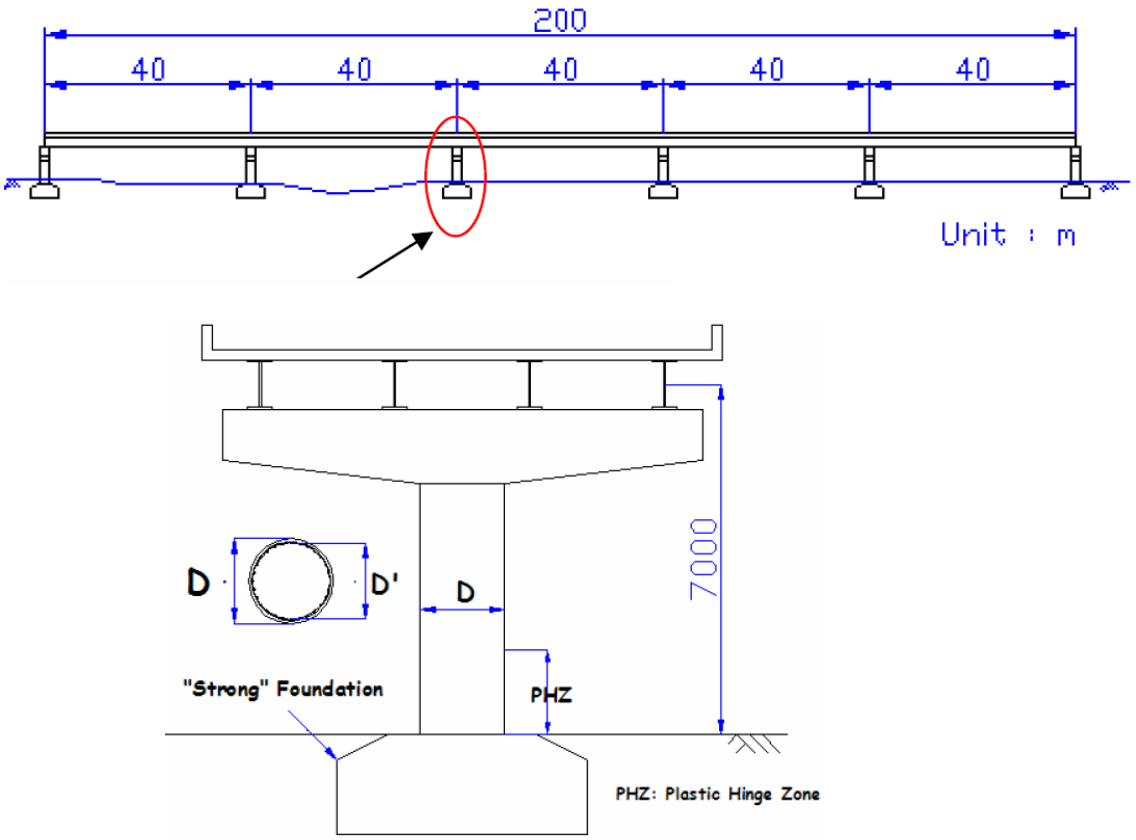

Figure 2. Bridge used in case study designed to New Zealand code provisions.
(Dhakal and Mander, 2006)

Table 1 presents the values of the key parameters for the case study bridge pier structure that is shown schematically in Figure 2. In Table 1, the parameter ρ_t represents the ratio of the longitudinal reinforcing bar cross-sectional area to the bridge pier's total cross-sectional area. Similarly, ρ_s represents the ratio of the volume of spiral reinforcing to the volume of the confined concrete.

Table 1. Key parameters of the Bridge Pier Case Study Structure.

Parameter	Value
D	1700 mm
D'	1540 mm
PHZ	1700 mm
$P/A_g f_c'$	0.15
Bar Details	28 @ D32
ρ_t	0.99%
Spiral	R20 @ 170mm
ρ_s	0.49%

3. RESULTS

3.1 Fatigue Damage Analysis

Figure 3 presents the results of individual time-history analyses using all eight available ground motion records from the Christchurch Central Business District (CBD) for the September 4th, 2010 main shock earthquake. The eight ground motions come from the two orthogonal horizontal directions from the four free-field GeoNet strong motion recording stations within the central city. Specifically, these stations are the Christchurch Botanic Gardens (CBGS), Christchurch Cathedral College (CCCC), Christchurch Hospital (CHHC), Resthaven (REHS).

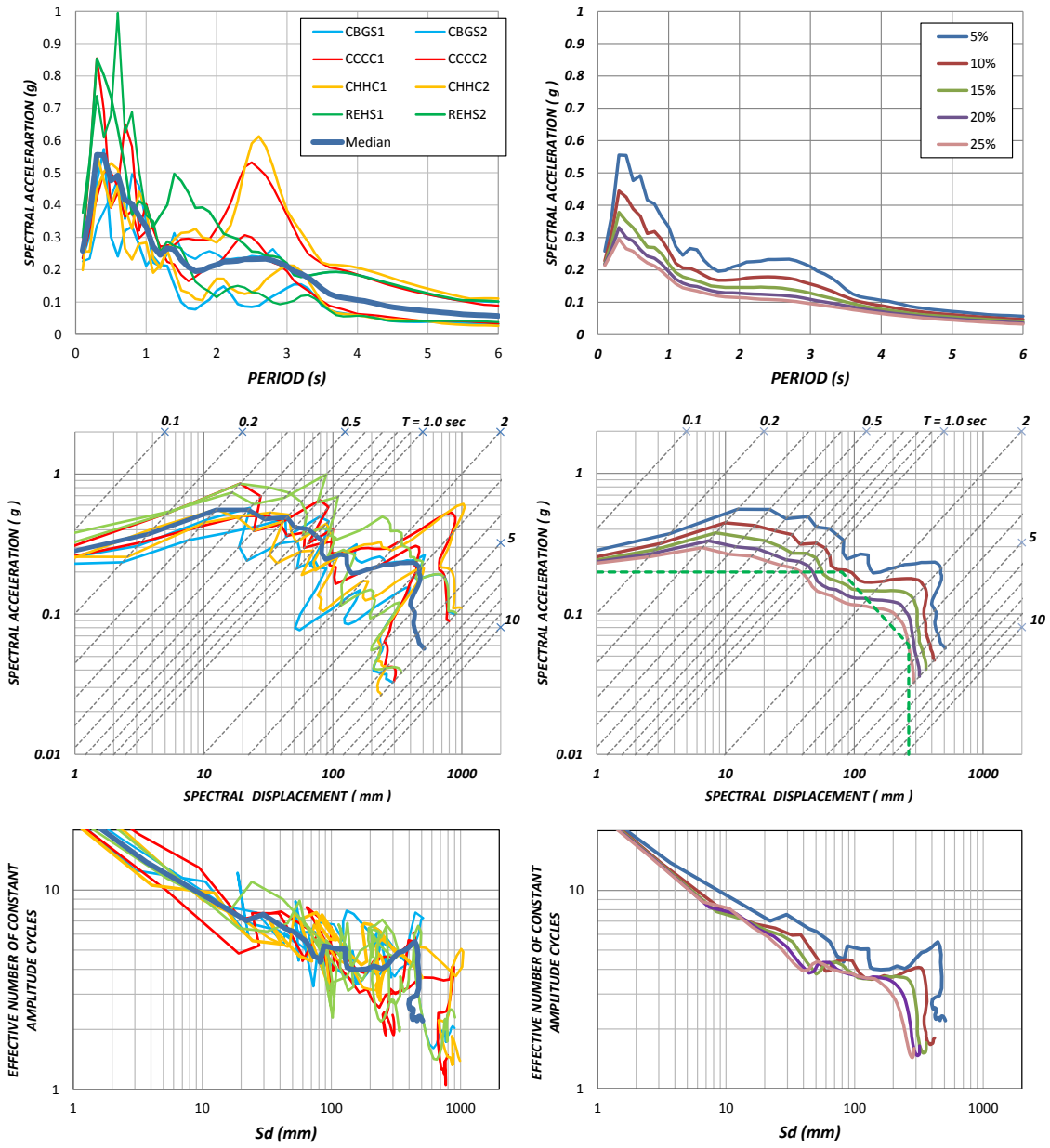

Figure 3. Response and cycle counting results for the September 4th, 2010 earthquake. The left column presents the results of individual time-history analyses with 5% inherent damping for all recorded ground motions, with the median result overlaid. The right column presents the median result for 5 levels of inherent damping.

The ground motions used in the time-history analyses were based upon the original accelerometer orientation and have not been corrected to a consistent North-South and East-West orientation. Elastic response spectra were generated for all eight ground motion recordings. The individual responses with 5% inherent structural damping are presented in the top left panel of Figure 3, along with the median response of these ground motions. The median response is used as a composite spectra whereby this single spectra is generated with known statistical (record-to-record variability) properties, instead of using all eight earthquake components individually, or any one component in isolation to draw conclusions. The use of this median response is intended to limit the chance of an erroneous conclusion being drawn from a single ground motion record which may not be representative of the typical ground shaking intensity experienced across the city. The use of a median spectra eliminates the need to have transformed the individual response history components into a consistent orientation, as it minimizes the effect of using the original instrument orientations.

The top right panel of Figure 3 presents the median acceleration response spectra from the eight ground motions for five levels of inherent structural damping, from 5% to 25% in increments of 5%. In the second row of Figure 3, the left column presents the eight individual ground motion responses with 5% inherent structural damping and the median of these results, but is now presented as an Acceleration-Displacement Response Spectra (ADRS) on log-log axes. The right column of the second row then presents the median response for the five levels of structural damping. Finally, the bottom row presents the effective number of constant amplitude cycles based upon the cycle counting method presented herein. Again, the left column represents the individual response components at 5% damping and the right panel represents the median response at different levels of inherent damping.

Subsequently, Figure 4 presents comparative results from the September 4th, 2010 and February 22nd, 2011 earthquakes. The left column of Figure 4 presents the same results that represent the fatigue demand that are included within Figure 3, but are now overlaid with the capacity curves to determine the performance point of the bridge structure. The upper row of graphs in Figure 4 presents the acceleration-displacement response spectra (ADRS) in log-log space for each earthquake event. In this way the diagonal lines plot the natural period of vibration for an elastic structure.

Also plotted on each ADRS graph as a thick red line in Figure 4 is the pushover capacity of the bridge pier such that the initial diagonal line falls on the natural period of the structure, while the horizontal plateau plots the plastic strength capacity. Over-plotted on the plastic capacity are blue bullets that show the response displacement amplitude for a prescribed level of equivalent viscous damping. The intersection of seismic demand and capacity gives the performance point denoted by the vertical dashed orange line with the spectral displacement (in mm) noted in red at the horizontal axis.

The second row of graphs in Figure 4 presents the results for the cyclic demand spectra computed using Eq. (10) with C = 2. The graph in the third row of Figure 4 shows the total cyclic demand for all earthquakes in the 2010-2011 Canterbury Earthquake Sequence. Note the results are normalized back to the maximum spectral displacement observed amongst all the earthquakes in the Sequence, as per Eq. (10), specifically the 22/2/2011 event; the largest earthquake in the Canterbury Earthquake Sequence.

Superimposed on the fatigue demand spectra graphs (in the second and third rows of Figure 4) is the cyclic fatigue capacity of the bridge structure represented by a thick diagonal red line. For a specified spectral amplitude, the red line provides the equivalent number of equi-amplitude cycles necessary to lead to first fatigue fracture of a longitudinal reinforcing bar in a pier column of the bridge. On that line is plotted an orange bullet and an associated number that indicates the *cyclic capacity* for that spectral displacement amplitude. Below that point at the same amplitude is a second orange coloured bullet point and number that represents the *cyclic demand* for the associated damping factor obtained from the ADRS graph above. The ratio of the *cyclic demand* to the *cyclic capacity* gives the fatigue damage fraction (D_f) with the results highlighted in yellow in the top right corner of each fatigue spectra graph.

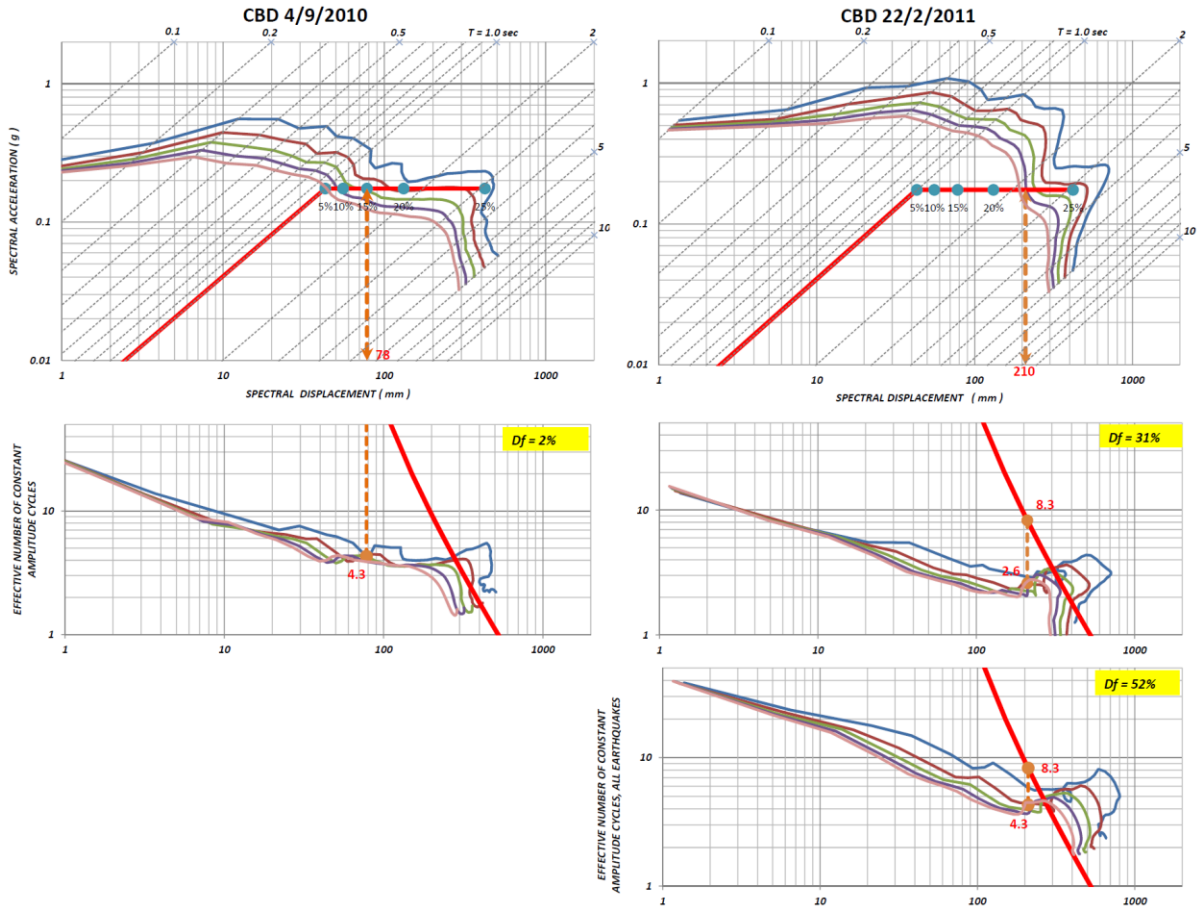

Figure 4. ADRS and Fatigue Spectra results for the bridge structure located within the vicinity of the Christchurch CBD subjected to the 2010-2011 Canterbury Earthquake Sequence

By using a single composite spectra as the median result, instead of using all eight earthquake components individually, or any one component in isolation, it is possible to obtain an estimate of the uncertainty in the ground motion input from the spread of the response. Thus, representative statistics were generated from individual ground motion response. The response quantities of this type of spectral analysis were assumed to conform to a log-normal distribution, characterized by two parameters: the median, $\hat{x}$; and the dispersion factor β (the log-normal standard deviation).

The spectral displacement and number of effective fully reversed cycles of loading (S_d, N_{eff}) are computed for each specified natural period and damping factor (T, ξ). Thus the spectral values plotted in Figure 4 are a median (the 50$_{th}$ percentile) of the 8 available components of motion.

Results of analyses of several structures have shown that reinforcement fatigue was mostly restricted to the four largest ground motion events of the 2010-2011 Canterbury Earthquake Sequence. However, a majority of the fatigue demand came from the 22/2/2011 M6.3 Lyttelton Earthquake ground motion. In Figure 4, the fatigue modelling for the 4/9/2010 Darfield event gives the damage for that event alone, whereas for the 22/2/2011 Lyttelton event the two fatigue spectra are normed back to the spectral displacements of that event, as required in Eq. (10). The upper fatigue spectra gives the damage for that event alone, whereas the bottom right spectra gives the computed number of constant amplitude cycles aggregated over all events in the Canterbury Earthquake Sequence.

For the initial Darfield Earthquake of 4/9/2010 shown in the left column of Figure 4, a spectral displacement of 78 mm is inferred at the intersection of the seismic demand and the structural capacity from the ADRS. This is equivalent to a ductility factor of μ =1.8 and a damage fraction of D_f=2% is inferred.

The largest earthquake in the CBD vicinity was the Lyttelton Earthquake of 22/2/2011 with the results shown in the right column of Figure 4. A displacement of 210 mm is inferred from the ADRS, implying a structure ductility factor of μ = 4.9. Using the associated fatigue spectra (right column, centre graph of Figure 4) a cyclic demand of 2.6 cycles is inferred for an associated fatigue capacity of 8.3 cycles. Thus for the main earthquake of 22/2/2011, a damage fraction of D_f=31% was consumed. However, if cycles over all damaging earthquakes in the Canterbury Earthquake Sequence are included from 4/9/2010 to 23/12/2011 are considered then the number of cycles increases from N_{eff} = 2.6 to 4.3 to give a total sequence damage fraction of D_f=52%.

3.2 interpretation of the fatigue analysis results including the effects of uncertainties

For a structure to be considered within a tight geographical region, such as the CBD of Christchurch (NZ), it was considered prudent to take a probabilistic approach whereby a single composite spectra is used with known statistical properties. Representative statistics were generated from the eight individual ground motion recordings for each earthquake event. The response quantities of this type of spectral analysis were shown to broadly conform to a log-normal distribution, and thus characterized by the two lognormal control parameters: the median and the log-normal standard deviation, which is also referred to herein as the dispersion factor β.

The dispersion for the total uncertainty in the analysis, β_T, is a combination of aleatory and epistemic uncertainties that are combined to give the total uncertainty in accordance with the methods established by Kennedy et al. (1980) and given by:

$$\beta_T = \sqrt{\beta_C^2 + \beta_D^2 + \beta_U^2} \tag{11}$$

in which β_C = the variability in the fatigue capacity of the reinforcing steel as shown by the scatter in the graphs of Figure 1; β_D = is the variability in the fatigue demand arising from the randomness in dynamic response and randomness in the effective number of computed cycles which is plotted for the entire spectra shown in the lower-right graph of Figure 4; and β_U = the epistemic uncertainty in the overall modelling approach taken herein as β_U = 0.35.

By using these values for β_C and β_U, and applying the spectral displacement for the lower right graph of Figure 4 to give β_T = 0.65, the total dispersion for the composite uncertainty given by Eq. (11) is β_T = 0.80.

Figure 5 presents the results for the uncertainties in terms of the bridge example for the 2010-2011 Df=1.0 plots the 'Fatigue Limit' fragility curve indicating that the fatigue life of the reinforcing steel may be consumed and fatigue cracks observable. The right most curve plots the 'Fatigue Fracture' fragility curve indicating the possibility fractures in the reinforcing steel may be observable.

The left most blue curve plots the fragility curve that represents the onset of irreparable damage. As low cycle fatigue damage to reinforcing steel in reinforced concrete structures cannot be restored, this curve is also defined as the "de minimis" condition. Note that damage to the left of that blue curve may not be sufficient to justify restoration.

In Figure 5 the fragility curves are plotted against two vertical lines, which are results from the fatigue damage analyses. The left (green) line is plotted at Df=33% and represents the total fatigue damage to the reinforcing steel in the pier columns of the bridge at the conclusion of the Earthquake of 22/2/2011. Following that main event there were numerous additional earthquakes, several of which were large and continued to inflict fatigue damage. The last of these, which defines the conclusion of the Earthquake Sequence occurred on 23/12/2011. The calculated damage of D_f = 52% is plotted as the right vertical line.

By examining the intersection of the vertical lines with the fragility curves it is possible to infer the 'probable damage states' of the bridge structure.

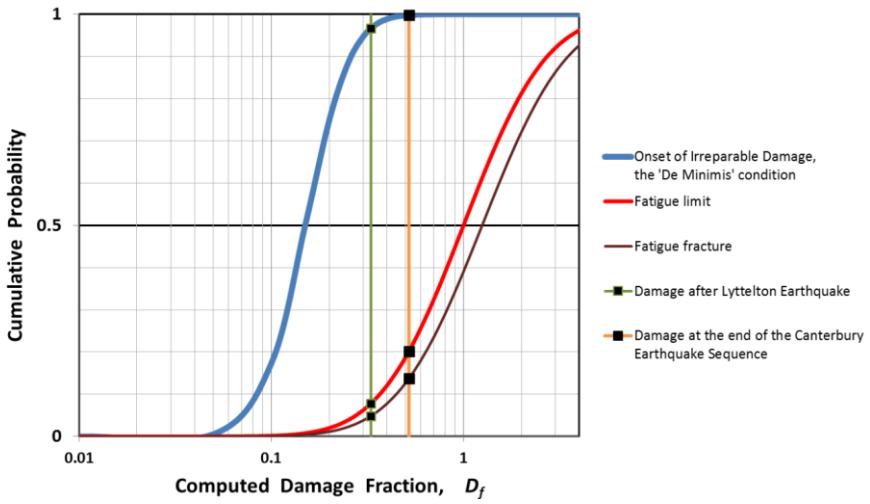

Figure 5. Fragility curves for reinforcing steel fatigue damage applied to the bridge during the Canterbury Earthquakes.

Supposing there were no more earthquakes following the Lyttelton event of 22/2/2010 then there is a 4.8% chance of rebar fractures in the piers. If however, the total consumption of fatigue life was considered, rather than mere fracture, this probability increases to 8.2% and a 96% chance that all steel had survived the *de minimis* condition. At this stage alone the bridge pier could be considered irreparable, and the pier would require reconstruction for full restoration.

Following the extremely strong earthquake of 22/2/2011 there were numerous earthquakes until the end of the sequence on 23/12/2011, three of which were strong events that incurred further low cycle fatigue damage, increasing the damage fraction from D_f=33% to 52%. When the orange vertical line in Figure 4 is plotted for D_f=52%, it intersects the fragility curve for fracture showing a 14% chance of fracture.

Also of importance is the fatigue limit, at which time the fatigue life is theoretically fully consumed with a 21% chance of occurrence. Finally, at the conclusion of the Earthquake Sequence the analysis shows there is a 99% probability that the *de minimis* condition is exceeded, confirming the bridge piers are irreparable requiring reconstruction for a full restoration to a substantially as new condition.

However, there may not be an extreme urgency for this repair as the ultimate safety against collapse has not been seriously impaired; rather the restoration is essential to assure long-term serviceability.

4. DISCUSSION AND CONCLUSIONS

New Zealand design codes have long recognised cyclic loading demands imposed by earthquakes and have historically required structures to be capable of sustaining four completely reversed cycles of inelastic loading with a structure ductility factor of four. Consequently, buildings and bridges are designed for reduced strength to a structure-specific loadings code. Concrete structures are then prescriptively detailed in their potential plastic hinge zones for ductility; such detailing has been validated through analysis and testing to ensure ductility capability under cyclic loading.

Not so well understood at the time these codes were written, is the problem of low cycle fatigue and its adverse effect on the longitudinal reinforcement in particular, as well as the confinement steel (Dutta and Mander, 2001). If a single earthquake occurs and causes noticeable damage, then it is also likely that the cyclic effect may have consumed some of the available fatigue resistance. Moreover, if several large earthquakes have occurred, the question of low-cycle fatigue becomes more prominent. If the structure has sustained significant fatigue damage, restoration to an as-new condition may be difficult.

As fatigue damage is irreparable, those damaged portions and their associated connections within the structure may be required to be rebuilt with new materials.

This paper has set forth a simple direct method of analysis to estimate the extent of low cycle fatigue damage to structures, and the longitudinal reinforcement in critical plastic hinge zones in particular, when subject to one or more earthquakes in a sequence.

To illustrate the fatigue analysis procedure and outcomes for the 2010-2011 Canterbury Earthquake Sequence, a case study of a simple bridge structure was presented for the Christchurch CBD. The inherent uncertainties in both the fatigue demand and resistance along with epistemic uncertainty associated with analysis simplifications were also considered.

The following overall conclusions are drawn:

1. For the Christchurch CBD, the initial Darfield event consumed only a minor (2%) fatigue life. If this were the only earthquake, such limited damage may be deemed *de minimis*, thereby not warranting restoration of that fatigue damage. However, the key Lyttelton earthquake of 2/22/2011 added another 30 percent fatigue damage, and by the end of the sequence this increased to 52 percent requiring restoration of that damage.
2. Results have been presented in the context of fatigue-based fragility curves. When D_f=52% there is a 14% chance of rebar fracture. Results show there is a 99% probability that the *de minimis* condition is exceeded, thereby confirming the bridge piers are irreparable, requiring reconstruction for a full restoration to a substantially as new condition.

7. REFERENCES

Brown, J., and Kunnath, S.K., (2004) Low-cycle fatigue failure of reinforcing steel bars. *ACI Materials Journal*, 101(6): 457-466.

Dhakal, R. P., and Mander, J. B., (2006) Financial loss estimation methodology for natural hazards *Bulletin of the New Zealand Society for Earthquake Engineering*, 39(2), 91-105.

Dutta, A., and Mander, J.B., (2001) Energy Based Methodology for Ductile Design of Concrete Columns *Journal of Structural Engineering, ASCE*, 127(12), 1374-1381.

Kennedy, R. P., Cornell, C. A., Campbell, R. D., Kaplan, S., & Perla, H. F. (1980). Probabilistic Seismic Safety Study of an Existing Nuclear Power Plant, *Nuclear Engineering and Design*, 59(2), 315-338. doi:10.1016/0029-5493(80)90203-4

Mander, J.B, Panthaki, F. and Kasalanati, A. (1994). Low-Cycle Fatigue Behavior of Reinforcing Steel. *Journal of Materials in Civil Engineering, ASCE*, 6(4): 453-468.

Tanabe, T., (1999). Comparative Performance of Seismic Design codes for Concrete Structures, Vol. 1, Elsevier, New York.